Geochemical Journal, Vol. 36, pp. 563 to 580, 2002

Mineral chemistry of barium- and titanium-bearing biotites in calc-alkaline volcanic rocks from the Mezitler area (Balıkesir-Dursunbey), western Turkey

FUAT YAVUZ,[1]* ALİ HAYDAR GÜLTEKİN,[1] YÜKSEL ÖRGÜN,[1] NURGÜL ÇELİK,[1]
MUAZZEZ ÇELİK KARAKAYA[2] and AHMET ŞAŞMAZ[3]

[1]İstanbul Teknik Üniversitesi, Maden Fakültesi, Maden Yatakları-Jeokimya Anabilim Dalı, 80670, Maslak, İstanbul, Turkey
[2]Selçuk Üniversitesi, Jeoloji Mühendisliği Bölümü, Mineraloji-Petrografi Anabilim Dalı TR-42031, Konya, Turkey
[3]Fırat Üniversitesi, Mühendislik Fakültesi, Jeoloji Mühendisliği Bölümü, 23100, Elazığ

(*Received October 5, 2001; Accepted May 31, 2002*)

Barium- and titanium-bearing biotites from Miocene volcanic rocks of Mezitler area, eastern Balıkesir, western Turkey are studied. The chemical composition of volcanic rocks range from andesite to rhyodacite. The iron-enrichment index of micas (average I.E. = 0.40) is intermediate between annite and phlogopite. The biotite phenocrysts contain up to 1.72 wt.% BaO and 5.90 wt.% TiO_2, with the average formulae $(K_{0.807}\,Na_{0.131}\,Ca_{0.036}\,Ba_{0.027})\,(Mg_{1.404}\,Fe^{2+}_{0.800}\,Fe^{3+}_{0.131}\,Ti_{0.303}\,Al_{0.056}\,Mn_{0.023})\,(Si_{2.832}\,Al_{1.167})\,O_{10}\,[(OH)_{1.976}\,Cl_{0.024}]$. The BaO content of electron-microprobe micas is positively correlated with the Al_2O_3, TiO_2, and FeO contents, and with the I.E., and is negatively correlated with the SiO_2, K_2O, and MgO contents. Ba- and Ti-rich micas are generally found in potassic igneous rocks, in subalkaline and alkaline gabbroic rocks and in contact metamorphic rocks, whereas Ba- and Ti-bearing micas in this study occur in calc-alkaline volcanic rocks that hosted manganese-oxide and barite deposits. Most of the phenocrysts analyzed have deficiencies in their octahedral and partly interlayer sites. Deficiencies in the octahedral sites may arise from the Ti-vacancy and partly the Ti-tschermakite substitution. On the other hand, deficiencies in the interlayer-site are due to the replacement of K by Ba. The substitution mechanism in the Mezitler micas is characterized by Ba + 2Ti + 3Al = (K+Na+Ca) + 3(Mg+Fe+Mn) + 3Si, with an excellent correlation coefficient. In terms of aluminum and titanium contents, micas from the Mezitler area lie on a similar trend parallel to that for metasomatic phlogopites from Canary Island xenoliths, which overlap the field for micas from the Ilha da Trindade xenolith, South Atlantic. Biotite compositions from the Mezitler area fall between the quartz-fayalite-magnetite (QFM) and nickel-nickel oxide (NNO) oxygen fugacity buffers. All these show that Mezitler micas with low to moderate Ba- and Ti-contents may be formed from magmas in a subduction-enriched sub-continental lithospheric mantle environment.

INTRODUCTION

Barian phlogopite and biotite occur most commonly in magmatic and contact metamorphic rocks including alkaline and peralkaline magmatic suites (Mansker *et al*., 1979), layered gabbroic calc-alkaline and alkaline rocks (Bigi *et al*., 1993; Shaw and Penczak, 1996) and calc-silicate rocks and marbles (Solie and Su, 1987; Bol *et al*., 1989; Tracy, 1991). Barium-rich phlogopite and biotite are commonly associated with high Ti, Fe, and Al and low Si, K, and Mg contents compared to Ba-poor micas (Edgar, 1992). In this respect, trioctahedral micas show substantially higher Ba concentrations compared to the dioctahedral counterparts, which occasionally have high in Cr and/or V contents (Grapes, 1993; Harlow, 1995). Mica compositions generally vary with temperature,

*Corresponding author (e-mail: yavuz@itu.edu.tr)

pressure, oxygen fugacity, fluid, and whole rock compositions. Understanding the factors that control the mica compositions is so far difficult. The Ti-content of micas, however, increases with increasing temperature, oxygen fugacity, decreasing pressure and decreasing water content of the system (Foley, 1990).

The study area is located in western Turkey, where widespread magmatic activity developed during the Oligocene to Middle Miocene. The volcanic activity produced intermediate to acid volcanic rocks such as andesite, rhyodacite, dacite and their tuffs; those, -and, to a lesser extent, limestone and marl, make up the geology of the Mezitler (Balıkesir-Dursunbey) area and its vicinity. On the basis of petrographic and geochemical studies, the majority of Miocene volcanic rocks are high-K calc-alkaline andesites. On the primitive mantle-normalized spider diagram, andesites are enriched in large-ion lithophile elements (LILE) over high-field strength elements (HFSE) and light rear earth elements (LREE), with the characteristics of orogenic magmatism. The behavior of trace-element concentration and their inter-element relationships suggest that the volcanic rocks were probably derived from magmas, which are generated in a subduction-enriched subcontinental lithospheric mantle. It is evident that the magma is also contaminated from the continental crust.

This paper describes the chemical composition of micas, their substitution mechanisms, paragenesis and petrogenesis from Miocene calc-alkaline rocks including andesite and, to a lesser extent, rhyodacite and dacite from the Mezitler area, where numerous vein-type manganese-oxide and barite deposits are hosted in volcanic rocks of western Turkey. Moderate- and high-Ti and Ba micas are found generally in alkaline magmatic rocks. However, we observed that low to modearte barium- and titanium-rich micas can be found associated with calc-alkaline magmatic rocks in western Turkey. The most consistent feature of the micas is a low to moderate Ba and Ti contents up to 1.72 wt.% BaO and 5.90 wt.% TiO_2 respectively.

GEOLOGY AND PETROGRAPHY

The Neogene geological evolution of western Turkey is characterized by a widespread magmatism. Three different rock associations can be recognized in the region respectively granitoids, an intermediate, and basic volcanic rocks. The granitoids are composed mostly of granodiorites, monzonites and to a lesser extent adamellites, leucogranites and syenites (Altunkaynak and Yılmaz 1995; Genç, 1995; Karacık and Yılmaz, 1995). The chemical composition of the intermediate volcanic rocks ranges from basaltic andesite to dacite, with dominant pyroclastics. These rocks show calc-alkaline geochemical affinities. The basic volcanic rocks are generally represented by basalts and subordinate mugearites, trachytes and hawaiites and hence, show alkaline geochemical behavior. During the late Paleocene and the early Eocene Pontides in the north collided with the Anatolide platform in the south. Due to this collision, western Anatolia, situated just to the west of Turkey, was subjected to a progressive compressional regime in north-south direction. Anatexis melting took place within the locally thickened continental crust with the aid of heat that transferred from mantle-derived melts along the subducted zone in western Anatolia. The continuation of subduction process until the Middle Eocene provided a source for the calc-alkaline magmas. A volcanic rock with different compositions such as rhyodacite, dacite, andesite, and basalt, was formed as a result of this mechanism from the Upper Oligocene to the end of the Pliocene (Ercan *et al.*, 1985; Genç and Yılmaz, 1995).

The geology of the Mezitler area is restricted to Miocene volcanic rocks of calc-alkaline association. The basement rocks of the vicinity area are biotite-muscovite schists, calc-schists and quartzites that lie within an area of Paleozoic metamorphic and metasedimentary rocks. There are numerous andesite-hosted vein-type Mn and Ba deposits in the Havran-Dursunbey metallogenic sub-province, eastern Balıkesir, western Turkey (Gültekin *et al.*, 1998; Gültekin

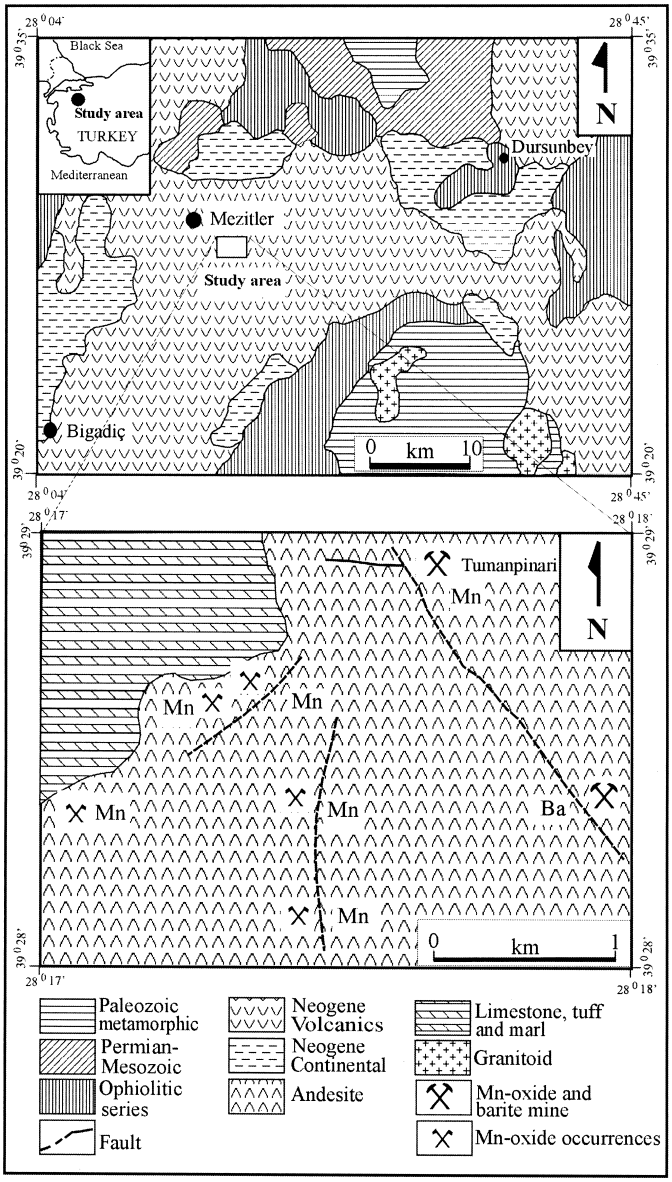

Fig. 1. Simplified geological map of the study area (modified from Ersoy, 1989).

and Örgün, 1999). The Mezitler area constitutes one of the most important Yalakkaya Mn-Ba deposits, which occur as Mn-oxide, barite veins, and lenses, along the steeply dipping northeast-trending faults (Fig. 1). Andesites are intensively altered to carbonate and clay minerals at the contacts of mineralization zones. Textural and mineralogical features in hydrothermally altered rocks provide a link between the alteration and mineralization processes (Gültekin and Örgün, 1999).

The mica phenocrysts are generally euhedral to subhedral and up to 4 mm in size, with dark reddish-brown color that is characteristic of Ba- and Ti-bearing micas. Mica phenocrysts show strongly pleochroic dark reddish-black rims. In some thin sections, rutile needles and apatite inclusions are observed at the dark-brown section of mica phenocrysts. The titanite/rutile-biotite

intergrowth, also referred to as the sagenitic texture, is characterized by slender, needle-like inclusions at an angle of 60° in a matrix included in mica, quartz, or other minerals. This type of occurrences may be formed through simple topotaxial precipitation from a parent solid solution phase (Shau *et al.*, 1991) or by inward diffusion of Ca and outward diffusion of Ti along the basal cleavage planes (Yui *et al.*, 2001). Groundmass micas show similar optical and chemical characteristics to those of the euhedral mica phenocrysts. Generally, no systematic zoning patterns have been detected. The micas contain apatite, zircon, plagioclase inclusions, and opaque minerals. Amphibole and pyroxene form euhedral to subhedral phenocrysts in porphyritic rocks. Opaque minerals associated with host rocks are magnetite, hematite, manganese-oxide and subordinate galena, sphalerite, chalcopyrite and pyrite. The groundmass of the volcanic rocks is composed largely of microlites of plagioclase associated commonly with lesser amount of sanidine. The average composition of plagioclase is $An_{45–50}$. The calc-alkaline volcanic rocks are porphyritic, with a hyalopilitic groundmass texture.

CHEMISTRY

The representative geochemical data for the volcanic rocks from Mezitler area are given in Table 1. The major, trace-, and rare-earth element contents of the samples were analysed by a commercial laboratory in Canada using inductively coupled plasma-atomic emission spectrometry (ICP-AES) and inductively neutron activation analysis (INAA) techniques. Sample splits of 1.0 gram are digested in a mixture of HNO_3, $HClO_4$, HF, and HCl acids at a high temperature. Then solutions including trace-element were analysed by ICP-AES. On the other hand, sample splits of 30 gram were irradiated and then analysed by INAA using gamma ray detection. Detection limits for each element for the ICP-AES and INAA techniques are given in Table 1. These rocks are mainly andesitic in composition, as is evident from

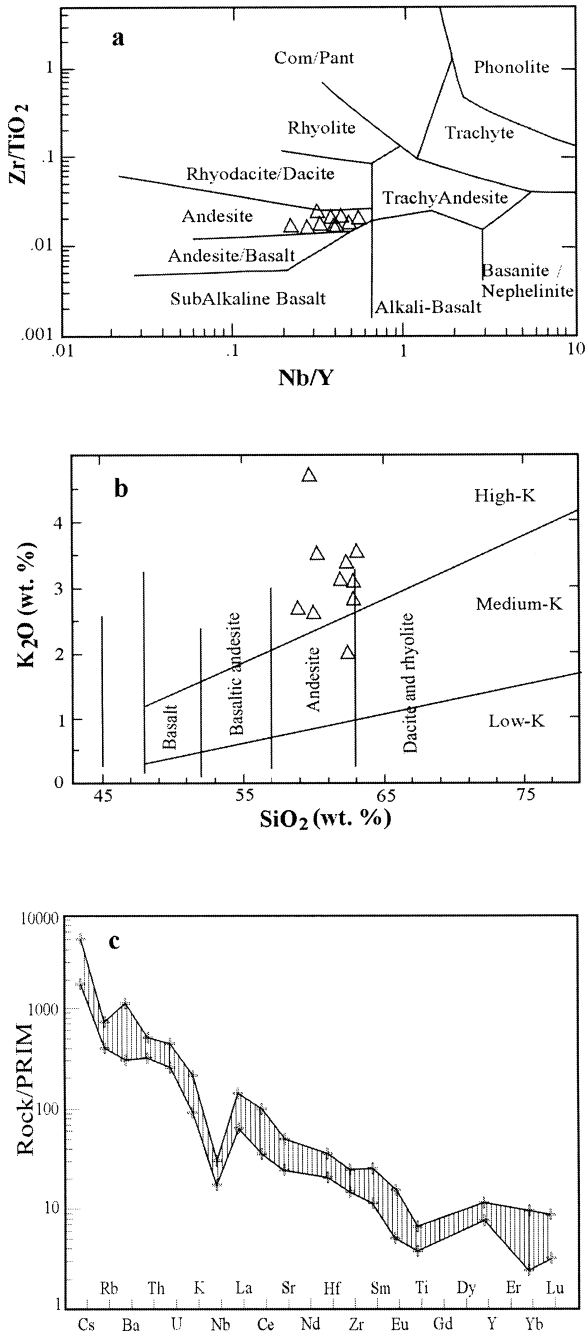

Fig. 2. a) Plot of volcanic rocks on Zr/TiO_2 - Nb/Y ratio diagram (fields after Winchester and Floyd, 1977). b) Position of samples on K_2O - SiO_2 variation diagram (fields after Le Maitre, 1989). c) Trace element concentrations normalized to the composition of primitive mantle.

Table 1. Major and trace element contents of volcanic rock containing Ba-bearing mica. Major oxides in wt. % and trace- and rare-earth elements in ppm.

	1	2	3	4	5	6	7	8	9	10
SiO_2	62.85	62.41	62.96	59.95	63.10	60.36	61.91	58.91	62.36	59.37
TiO_2	0.60	0.74	0.85	0.62	0.65	0.84	0.70	0.63	0.49	0.73
Al_2O_3	13.61	16.63	15.92	18.13	17.18	16.52	16.09	14.87	17.51	15.69
$Fe_2O_{3(tot)}$	6.81	5.88	7.98	4.53	5.12	6.21	5.98	6.84	5.20	5.96
MnO	0.08	0.13	0.15	0.05	0.03	0.96	0.20	0.11	0.13	0.10
MgO	1.39	1.53	0.79	1.29	1.69	1.74	0.98	3.57	1.46	1.80
CaO	5.60	3.80	2.91	6.70	2.90	4.71	7.04	5.93	3.98	5.52
Na_2O	3.03	5.07	3.17	2.23	4.45	2.62	2.48	3.18	2.44	2.34
K_2O	3.06	1.97	2.82	3.52	2.60	3.51	3.10	2.66	3.37	4.83
P_2O_5	0.13	0.05	0.10	0.12	0.16	0.36	0.14	0.42	0.20	0.26
BaO	0.21	0.17	0.28	0.16	0.15	0.48	0.17	0.18	0.15	0.55
LOI	1.43	1.25	1.96	2.19	2.04	2.60	0.90	2.09	2.37	2.75
Total	98.80	99.63	99.89	99.49	100.07	100.91	99.69	99.39	99.66	99.90
Sc	18	14	12	14	12	13	10	14	13	17
V	110	192	150	192	114	94	68	180	70	94
Cr	39	18	28	18	32	10	17	36	28	21
Co	20	13	21	13	22	16	6	16	12	14
Ni	40	49	43	38	50	37	33	48	39	42
Rb	230	190	170	190	280	168	203	200	250	198
Sr	556	545	622	545	325	612	452	550	480	650
Y	26	25	20	25	22	23	26	29	30	22
Zr	145	128	147	128	131	151	169	110	100	151
Nb	8	10	8	10	10	9	11	9	13	9
Cs	18	23	9	23	18	19	21	12	26	19
La	57	51	35	51	50	60	29	58	49	51
Ce	110	80	79	80	79	94	40	72	105	61
Sm	6.40	4.90	6.70	4.89	3.80	3.19	n.d.	3.80	5.70	4.90
Eu	1.50	1.20	1.52	1.15	0.52	0.81	n.d.	1.2	1.4	1.3
Yb	2.70	2.10	2.81	2.06	0.72	1.38	n.d.	2.4	2.7	2.1
Lu	0.39	0.30	0.38	0.27	0.14	0.16	n.d.	0.34	0.39	0.30
Hf	7	5	4	5	5	4	7	6	7	6
Ta	0.2	1	1.2	1	1	1	1.8	0.9	0.7	1
Pb	395	120	900	120	696	500	294	420	390	740
Th	30	24	20	24	26	23	22	24	30	21
U	7	6	4	6	5	6	4	5.9	4.5	6.3

n.d.: not determined. Detection limits (ppm): Lu (0.05); Sm, Ta (0.1); Eu, Yb (0.2); U (0.5); Sc, Cs, Hf (1); V, Cr, Co, Ni, Sr, Y, Zr, Nb, La, Th (2); Ce (3); Pb (5); Rb (15).

the Zr/TiO_2 vs. Nb/Y ratio diagram of Winchester and Floyd (1977), which is shown in Fig. 2a. The range of andesite composition spans the medium-K to high-K fields on the classification diagram of Le Maitre (1989) (Fig. 2b). The volcanic rocks are moderate to strongly enriched in highly incompatible elements, whereas depleted in compatible elements. On the primitive mantle-normalized diagram, andesites are enriched in LILE with respect to LREE and HFSE and depleted in HFSE with respect to neighboring on LILE and LREE (Fig. 2c). All these are the characteristics of orogenic magmatism and convergent margin magmas. All mica (except for sagenitic biotite) and coexisting mineral analyses were made at the laboratory of Metallurgy Engineering, İstanbul Technical University, using wavelength-dispersion spectrometry (WDS) on a JEOL JSM-840 scanning microscope at an accelerating voltage of 15 kV, beam current of 10 nA, 5-μm electron beam, and a ZAF correction scheme. Natural minerals and synthetic compounds were used as standards. Benitoite

Table 2. Results of electron-microprobe analyses of representative biotite phenocrysts from Mezitler area, western Turkey

	1	2	3	4	5	6	7	8	9
SiO_2	38.62	38.50	37.09	37.01	37.58	37.80	38.10	38.45	38.20
TiO_2	4.43	4.97	5.83	5.78	5.53	5.63	5.48	5.01	5.36
Al_2O_3	13.31	13.38	14.6	14.29	14.15	14.1	13.86	13.43	13.75
FeO	13.94	14.37	15.55	15.31	15.28	15.26	15.10	14.50	14.83
MnO	0.51	0.47	0.18	0.22	0.33	0.37	0.36	0.45	0.41
MgO	13.1	12.88	12.23	12.12	12.42	12.50	12.69	12.84	12.68
BaO	0.40	0.48	1.68	1.55	1.34	1.05	0.76	0.51	0.63
CaO	0.78	0.72	0.14	0.21	0.32	0.38	0.52	0.67	0.56
Na_2O	1.33	1.24	0.58	0.64	0.76	0.80	0.93	1.20	0.96
K_2O	9.02	8.84	8.10	8.16	8.25	8.25	8.57	8.57	8.63
Cl	0.04	0.07	0.37	0.33	0.25	0.21	0.20	0.09	0.10
Total	95.48	95.92	96.35	95.62	96.21	96.35	96.57	95.72	96.11
Si	2.89	2.87	2.78	2.79	2.81	2.82	2.83	2.87	2.84
Al^{IV}	1.11	1.13	1.22	1.21	1.19	1.18	1.17	1.13	1.16
Total (T)	4.00	4.00	4.00	4.00	4.00	4.00	4.00	4.00	4.00
Al^{VI}	0.06	0.05	0.07	0.07	0.06	0.06	0.05	0.05	0.05
Ti	0.25	0.28	0.33	0.33	0.31	0.32	0.31	0.28	0.30
Fe^{2+}	0.64	0.78	0.73	0.77	0.81	0.80	0.86	0.83	0.90
Fe^{3+}	0.23	0.12	0.25	0.20	0.14	0.15	0.07	0.07	0.03
Mn	0.03	0.03	0.01	0.01	0.02	0.02	0.02	0.03	0.03
Mg	1.46	1.43	1.37	1.36	1.39	1.39	1.41	1.43	1.41
Total (M)	2.91	2.91	2.92	2.9	2.92	2.93	2.93	2.92	2.92
Ba	0.01	0.01	0.05	0.05	0.04	0.03	0.02	0.01	0.02
Ca	0.06	0.06	0.01	0.02	0.03	0.03	0.04	0.05	0.04
Na	0.19	0.18	0.08	0.09	0.11	0.12	0.11	0.17	0.14
K	0.86	0.84	0.77	0.79	0.79	0.78	0.81	0.82	0.82
Total (I)	1.13	1.09	0.92	0.94	0.96	0.96	1.01	1.06	1.02
Cl	0.01	0.01	0.05	0.04	0.03	0.03	0.03	0.01	0.01
OH	1.99	1.99	1.95	1.96	1.97	1.97	1.97	1.99	1.99
Total (A)	2.00	2.00	2.00	2.00	2.00	2.00	2.00	2.00	2.00
X_{ph}	0.503	0.493	0.468	0.47	0.474	0.474	0.481	0.490	0.48
X_{an}	0.222	0.267	0.249	0.264	0.278	0.272	0.295	0.286	0.30
X_{pdo}	0.157	0.118	0.142	0.125	0.113	0.119	0.096	0.101	0.08
X_{mn}	0.011	0.010	0.004	0.005	0.007	0.008	0.008	0.010	0.00
X_{al}	0.021	0.016	0.025	0.023	0.021	0.019	0.016	0.018	0.01
X_{ti}	0.086	0.096	0.113	0.113	0.107	0.108	0.105	0.096	0.10
I.E.	0.38	0.39	0.42	0.42	0.41	0.41	0.41	0.4	0.4
Mg#	0.63	0.62	0.58	0.59	0.59	0.59	0.6	0.61	0.6
$Fe^{2+}/(Fe^{2+}+Fe^{3+})$	0.739	0.867	0.744	0.791	0.849	0.837	0.921	0.921	0.97
Talc	0.000	0.000	8.012	5.747	3.675	3.874	0.000	0.000	0.00
Ti-phlogopite	24.915	27.866	32.879	32.819	31.135	31.563	30.627	28.123	30.02
Ferri-eastonite	22.719	11.9	24.954	20.161	14.477	15.496	7.451	7.194	2.80
Muscovite	18.933	9.917	4.159	3.36	2.413	2.583	1.242	5.995	0.46
Eastonite	0.000	0.000	0.000	0.000	1.367	0.500	2.055	0.000	4.24
Phlogopite	33.433	50.318	29.996	37.913	46.934	45.984	58.625	58.688	62.46

Table 2. (continued)

	10	11	12	13	14	15	16	17	18
SiO_2	37.88	37.95	38.33	37.49	38.23	38.40	38.58	38.29	36.88
TiO_2	5.59	5.52	5.50	5.68	5.53	5.13	4.80	5.30	5.90
Al_2O_3	14.01	13.93	14.05	14.34	13.92	13.55	13.34	13.68	14.68
FeO	15.14	15.02	14.97	15.4	15.13	14.64	14.21	14.72	15.68
MnO	0.40	0.42	0.38	0.26	0.34	0.46	0.49	0.44	0.16
MgO	12.56	12.63	12.76	12.4	12.73	12.80	13.05	12.64	12.16
BaO	0.90	0.85	0.65	1.20	1.30	0.56	0.44	0.60	1.72
CaO	0.41	0.46	0.45	0.26	0.44	0.66	0.64	0.62	0.10
Na_2O	0.84	0.89	0.79	0.69	0.85	1.14	1.31	1.09	0.51
K_2O	8.33	8.45	8.74	8.50	8.21	8.54	8.76	8.89	8.04
Cl	0.18	0.16	0.14	0.28	0.23	0.10	0.06	0.11	0.44
Total	96.24	96.28	96.76	96.5	96.91	95.98	95.68	96.38	96.27
Si	2.82	2.83	2.84	2.8	2.83	2.86	2.88	2.85	2.77
Al^{IV}	1.18	1.17	1.16	1.2	1.17	1.14	1.12	1.15	1.23
Total (T)	4.00	4.00	4.00	4.00	4.00	4.00	4.00	4.00	4.00
Al^{VI}	0.05	0.05	0.06	0.06	0.05	0.05	0.05	0.05	0.07
Ti	0.31	0.31	0.31	0.32	0.31	0.29	0.27	0.3	0.33
Fe^{2+}	0.81	0.83	0.84	0.79	0.83	0.87	0.76	0.87	0.69
Fe^{3+}	0.14	0.1	0.09	0.18	0.1	0.04	0.12	0.04	0.29
Mn	0.03	0.03	0.02	0.02	0.02	0.03	0.03	0.03	0.01
Mg	1.40	1.40	1.41	1.38	1.41	1.42	1.45	1.40	1.36
Total (M)	2.93	2.93	2.94	2.92	2.94	2.92	2.92	2.9	2.92
Ba	0.03	0.02	0.02	0.04	0.04	0.02	0.01	0.02	0.05
Ca	0.03	0.04	0.04	0.02	0.03	0.05	0.05	0.05	0.01
Na	0.12	0.13	0.11	0.1	0.12	0.16	0.19	0.16	0.07
K	0.79	0.8	0.82	0.81	0.78	0.81	0.83	0.84	0.77
Total (I)	0.97	0.99	0.99	0.97	0.97	1.05	1.09	1.07	0.90
Cl	0.02	0.02	0.02	0.04	0.03	0.01	0.01	0.01	0.06
OH	1.98	1.98	1.98	1.96	1.97	1.99	1.99	1.99	1.94
Total (A)	2.00	2.00	2.00	2.00	2.00	2.00	2.00	2.00	2.00
X_{ph}	0.476	0.479	0.479	0.473	0.479	0.487	0.497	0.483	0.467
X_{an}	0.276	0.285	0.286	0.269	0.284	0.299	0.262	0.300	0.238
X_{pdo}	0.114	0.103	0.103	0.122	0.108	0.088	0.120	0.089	0.153
X_{mn}	0.009	0.009	0.008	0.006	0.007	0.010	0.011	0.010	0.003
X_{al}	0.018	0.017	0.02	0.021	0.017	0.017	0.018	0.016	0.025
X_{ti}	0.107	0.106	0.104	0.109	0.105	0.098	0.092	0.102	0.114
I.E.	0.410	0.410	0.400	0.410	0.410	0.400	0.390	0.400	0.420
Mg#	0.600	0.600	0.600	0.590	0.600	0.610	0.620	0.600	0.580
$Fe^{2+}/(Fe^{2+}+Fe^{3+})$	0.856	0.892	0.907	0.818	0.889	0.959	0.862	0.951	0.705
Talc	2.746	0.678	0.742	3.435	2.84	0.000	0.000	0.000	9.611
Ti-phlogopite	31.335	30.927	30.595	31.900	30.838	28.74	26.933	29.647	33.346
Ferri-eastonite	13.628	10.152	8.648	17.541	10.441	3.756	12.211	4.476	29.069
Muscovite	2.271	1.692	1.441	2.924	1.740	3.130	10.176	3.730	4.845
Eastonite	0.877	1.654	3.128	0.339	1.653	0.000	0.000	0.000	0.000
Phlogopite	49.142	54.896	55.445	43.861	52.489	64.374	50.68	62.146	23.129

Note: T, M, I, and A are abbreviations for tetrahedral cations, octahedral cations, interlayer cations, and anions proposed by the IMA nomenclature for micas (Rieder, 2001). X_{ph}, X_{an}, X_{pdo}, X_{mn}, X_{al}, X_{ti} = Mole fractions of phlogopite, annite, proton-deficient oxyannite, manganobiotite, aluminobiotite and titanobiotite determined on basis of all octahedral ions (calculations from Jacobs and Parry 1979). Iron-enrichment index (I.E.) = (Fe+Mn)/(Fe+Mn+Mg). Magnesium number (Mg#) = Mg/(Mg+Fe). Ferric and ferrous iron separation is obtained by the Bioterm software (Yavuz and Öztaş, 1997). Mica variety is identified on the classification scheme by Tischendorf et al. (1997) using the Limica (Yavuz, 2001a) software. Mica end-member calculations (wt.%) as talc, Ti-phlogopite, ferri-eastonite, muscovite, eastonite, and phlogopite are taken from Dymek (1983).

Table 3. Representative compositions of minerals coexisting with mica in andesitesftom the Mezitle area

	1	2	3	4	5	6	7	8	9
SiO_2	41.28	43.23	42.45	55.48	51.24	53.58	57.01	54.07	56.58
TiO_2	3.35	3.08	2.60	0.21	1.11	0.28	0.00	0.00	0.00
Al_2O_3	13.86	11.99	12.79	9.20	5.36	2.05	26.80	25.89	27.24
Cr_2O_3	0.00	0.00	0.00	0.00	0.00	0.65	0.00	0.46	0.00
FeO	10.99	12.89	12.19	5.45	6.88	4.59	0.93	0.16	0.24
MnO	0.17	0.23	0.30	0.00	0.00	0.00	0.00	0.00	0.00
MgO	12.69	11.13	10.29	8.36	12.92	15.23	0.00	0.00	0.00
CaO	11.13	10.79	12.14	18.29	21.10	22.90	9.71	13.54	9.18
Na_2O	2.23	2.53	2.01	1.86	0.98	0.53	4.62	4.99	5.38
K_2O	1.73	1.60	1.62	0.64	0.21	0.00	0.65	0.58	0.55
Cl	0.16	0.16	0.20	0.00	0.00	0.00	0.00	0.00	0.00
Total	97.59	97.63	96.74	99.49	99.80	99.81	99.72	99.69	99.17
	23(O)	23(O)	23(O)	6(O)	6(O)	6(O)	8(O)	8(O)	8(O)
Si	6.07	6.42	6.37	2.06	1.90	1.97	2.57	2.48	2.56
Al	2.40	2.10	2.26	0.40	0.23	0.09	1.43	1.52	1.44
Ti	0.37	0.34	0.29	0.01	0.03	0.01	0.00	0.00	0.00
Cr	0.00	0.00	0.00	0.00	0.00	0.02	0.00	0.00	0.00
Fe^{2+}	1.11	1.60	1.53	0.17	0.21	0.14	0.04	0.02	0.01
Fe^{3+}	0.24	0.00	0.00	0.00	0.00	0.00	0.00	0.00	0.00
Mn	0.02	0.03	0.04	0.00	0.00	0.00	0.00	0.01	0.00
Mg	2.78	2.46	2.30	0.46	0.71	0.83	0.00	0.00	0.00
Ca	1.75	1.72	1.95	0.73	0.84	0.90	0.47	0.67	0.45
Na	0.64	0.73	0.59	0.13	0.07	0.04	0.40	0.44	0.47
K	0.32	0.30	0.31	0.03	0.01	0.00	0.04	0.03	0.03
Cl	0.04	0.04	0.05	0.00	0.00	0.00	0.00	0.00	0.00
Mg#	0.67	0.61	0.60	0.73	0.77	0.85	—	—	—
An%	—	—	—	—	—	—	51.53	58.21	46.89

Minerals: 1 = Potassian-titanian pargasite, 2 = Potassian-titanian pargasite, 3 = Potassian-titanian pargasite, 4 = Aluminian-ferroan-sodian diopside, 5 = Aluminian-ferroan diopside, 6 = Chromian-ferroan diopside, 7, 8, 9 = Plagioclase. The Newamphcal (Yavuz, 1999) and Pyrox (Yavuz, 2001b) softwares were used for calculations of amphibole and pyroxene samples.

($BaTiSi_3O_9$) was used to evaluate the overlap between the Ba$L\alpha_1$ and Ti$K\alpha_1$ lines. Benitoite analyses gave BaO 37.13–38.41 wt.%, TiO_2 18.38–18.89 wt.%, and SiO_2 43.35–43.46 wt.%. These results indicate that error due to overlap of Ba and Ti peaks is minimal and there exists a good agreement between analyses and theoretical values.

Analyses and cell formulae of representative mica and the coexisting minerals from the Mezitler area are given in Table 2 and in Table 3, respectively. The BIOTERM (Yavuz and Öztaş, 1997), LIMICA (Yavuz, 2001a) and MICA$^+$ (2002) computer programs are used for mineralogical calculations of the mica analyses. Analyzed mica samples have Mg# [Mg/(Mg+Fe)] < 0.66. In that way, biotites may have crystallized from a more evolved calc-alkaline magma compared to micas from alkaline potassic rocks. All of the phenocrysts lie within the eastonite-siderophyllite-phlogopite-annite field. The sample with the highest BaO content, however, is close to the phlogopite sector. Figure 3a is a plot of the octahedrally coordinated cations in terms of Foster (1960) showing the fields of different types of micas. Biotites plot on the line along which Mg: Fe ratio is 1:1. Micas are classified as Fe- and Mg-biotites on the classification diagram (Fig. 3b) proposed by Tischendorf *et al.* (1997). The biotites show compositions with SiO_2 = 36.88–38.62 wt.%, FeO = 13.94–15.68 wt.%, Al_2O_3 = 13.31–14.68 wt.%, K_2O = 8.04–9.02 wt.%, TiO_2 = 4.43–5.90 wt.%, BaO = 0.40–1.72 wt.% and Mg# [Mg# = Mg/(Mg+Fe)] = 0.58–0.63. They contain up to 0.44 wt.% Cl (see Table 2).

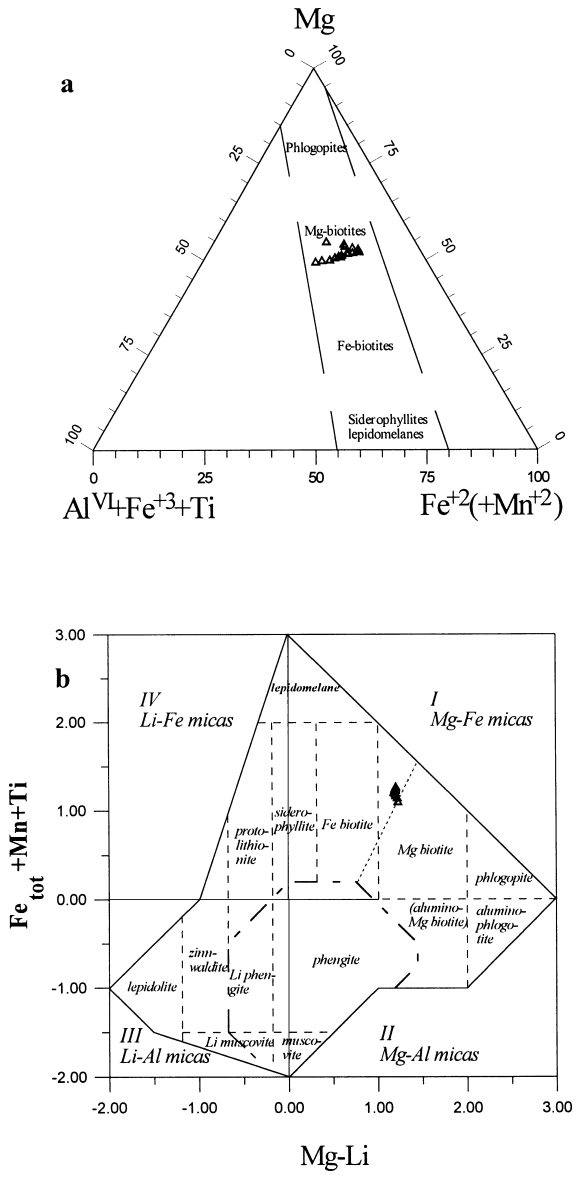

Fig. 3. a) Distribution of mica samples in the octahedral ion diagram of Foster (1960). b) Position of trioctahedral micas in the mica classification diagram of Tischendorf et al. (1997).

Structural formulae calculated on the basis of 22 positive charges show that Si and Al cation p.f.u. generally fill the tetrahedral sites. The octahedral sites, however, display slightly more variability between 2.90 to 2.92 cations p.f.u. (average 2.22 p.f.u.). The 12-fold co-ordination sites range between 0.90 to 1.13, with an average of 1.00 cation p.f.u. All these indicate that micas are close to the ideal stoichiometric values. Figure 4 shows that with increasing BaO there is a systematic decrease in SiO_2, K_2O, and MgO and increase in Al_2O_3, TiO_2, and FeO. The trends in Fig. 4 are similar to those for the more BaO and TiO_2 rich micas from the Hawaiian nephelinites (Mansker *et al*., 1979), from the West Eifel alkali mafic lavas (Edgar, 1992), and from the barian-titanian micas in a lamprophyric dyke from Ilha da Trindade (Greenwood, 1998). A comparison between the barian-titanian biotites from the Mezitler area with those from the West Eifel (Edgar, 1992), from the Brome alkaline igneous complex (Henderson and Foland, 1996), and from Ilha da Trindade (Greenwood, 1998) indicates a lower compositional range in BaO, TiO_2, Al_2O_3, MgO and a greater compositional range in SiO_2, K_2O, Na_2O, CaO, MnO and FeO. The BaO (wt.%) values of Mezitler rocks range between 0.15 to 3.03 and increases towards the altered andesites, with extensive silicification, up to 6.35 wt.% (Table 1). It appears that Ba-bearing biotites from this region reflect the Ba contents of their host rocks. This result agrees with the experimental study of Foley (1989), who suggested that Ba-rich micas also reflect high Ba values in their host rocks.

The composition of coexisting clinopyroxene has the highest Mg#, with the range of 0.71 to 0.86 (average Mg# = 0.78) compared to amphibole (average Mg# = 0.64) and biotite (average Mg# = 0.60). The amphibole is most commonly potassian-titanian pargasite. The coexisting clinopyroxene is generally aluminian-ferroan-sodian diopside (Table 3). The An contents of plagioclase range from 0.50 to 0.58 (average An% = 50.67), which agree with the Mg# values of the coexisting biotites and amphiboles.

DISCUSSION

Ba substitutions

It is difficult do assign a unique substitution mechanism for barium- and titanium-bearing micas because of the complexity of potential substi-

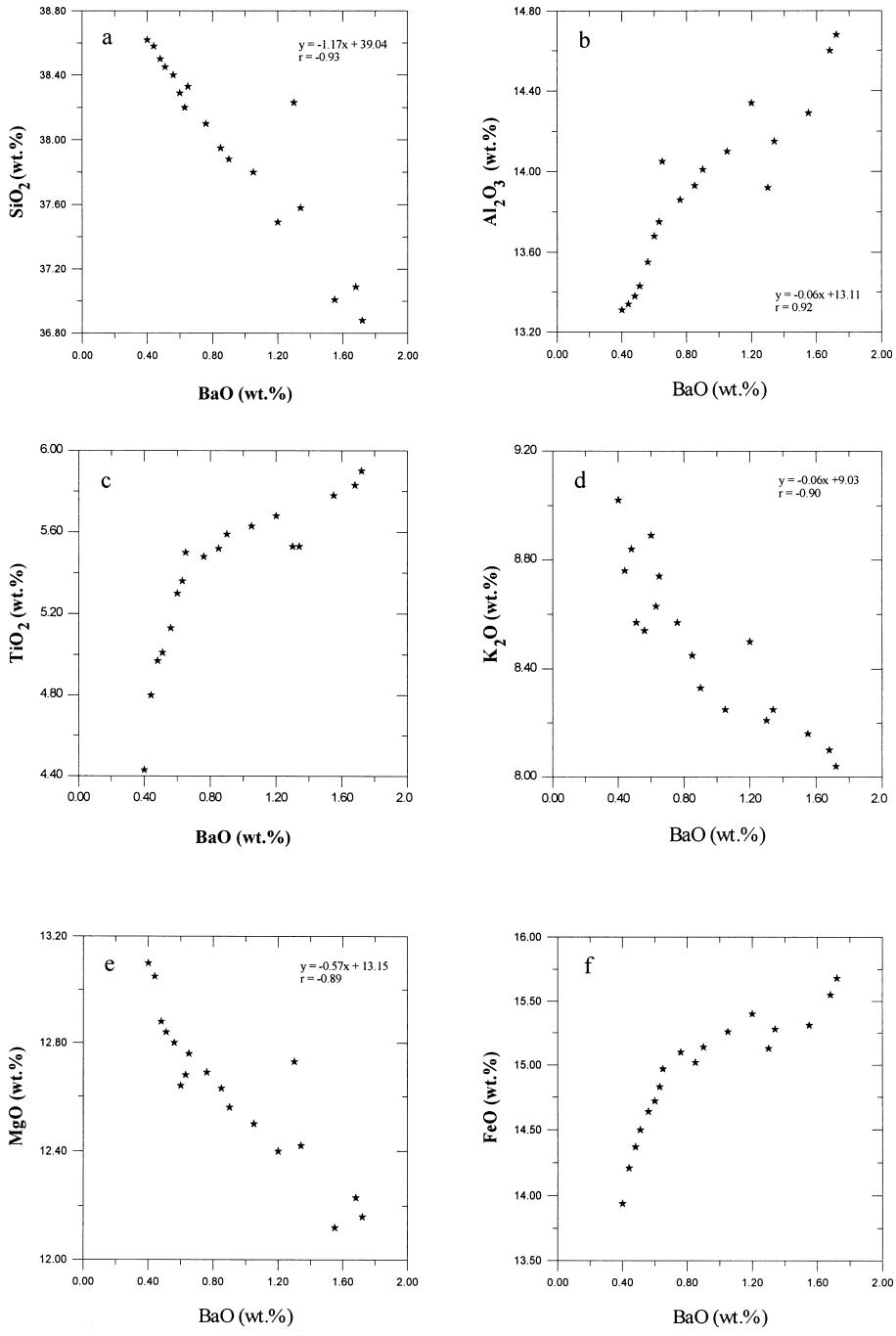

Fig. 4. Variation of the contents of selected oxides with BaO contents for micas from the Mezitler area.

tutions, the problems in determining valence of Fe and Ti, and the possibility of Ti, Fe and Mg in tetrahedral co-ordination (Foley, 1990; Zhang *et al*., 1993; Shaw and Penczak, 1996). However, some knowledge on interatomic correlations helps to identify the exchange components and valid substitutions. The exchange mechanisms for the Ba-bearing large cations can be generalized as the following equation:

$$Ba^{2+} + {}^{[j]}A^{x} \leftrightarrow (K^{+}, Na^{+}) + {}^{[j]}B^{x+1} \qquad (1)$$

where A and B can be cations, anions, or a vacancy (□), in the mica structural formulae, *j* is the coordination number of the coupled site, and *x* is the ionic charge (Harlow, 1995). Several investigators (e.g., Mansker *et al*., 1979; Guo and Green, 1990; Edgar, 1992; Zhang *et al*., 1993; Shaw and Penczak, 1996; Henderson and Foland, 1996; Greenwood, 1998) discussed the principal substitutions in barium-bearing micas. There are several alternative substitutions involving Ba within the interlayer-site on the mica structure. Mitchell (1981), Wagner and Velde (1986), and Guo and Green (1990) proposed Ba substitution for interlayer cations in the 12-fold site in micas. Correlation between BaO and K_2O indicates that the replacement of K by Ba in the mica structure needs charge compensation by a substitution given below.

$$^{[12]}Ba + \square = 2\ ^{[12]}K. \qquad (2)$$

Replacement of Ba by complex coupled substitutions involving cations from both the octahedral and interlayer site was proposed by Wendlandt (1977), Mansker *et al*. (1979), and Bol *et al*. (1989) by the following equation.

$$^{[12]}Ba + {}^{[4]}Al = {}^{[12]}K + {}^{[4]}Si. \qquad (3)$$

Replacement of K^{1+} by Ba^{2+} in the interlayer-site requires a charge compensation that needs different cations in tetrahedral or octahedral co-ordination or vacancies in the interlayer-site (Speer, 1984).

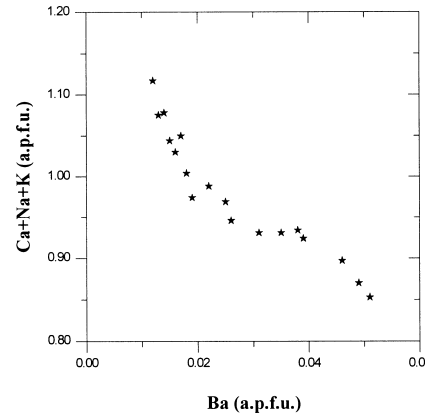

Fig. 5. Plot of mica compositions from the Mezitler rocks on a Ca+Na+K vs. Ba diagram.

Biotite compositions from the Mezitler area have low interlayer-site occupancies (Table 2), showing the presence of vacancies. The decrease in K_2O and SiO_2 with increasing BaO and Al_2O_3 (Figs. 4a, b and d) indicates that the coupled substitution (3) may be applicable to the Mezitler micas. However, this type of substitution does not explain the overall-compositional variation, and a more complex coupled substitution may be taken into account. The correlation coefficient ($r = 0.93$) between K+Na+Ca vs. Ba (Fig. 5) for biotites supports that Ba occurs in the 12-fold interlayer site. Other complex coupled substitutions were proposed by Mansker *et al*. (1979) and Velde (1979), which are applicable to micas from Mezitler rocks plotted in Figs. 6a, b and c.

$$^{[12]}Ba + 3\ ^{[6]}Ti + 4\ ^{[4]}Al = 2\ ^{[12]}K + 4\ ^{[6]}(Mg+Fe) + 4\ ^{[4]}Si \qquad (4)$$

$$^{[12]}Ba + 2\ ^{[6]}Ti + 3\ ^{[4]}Al = {}^{[12]}K + 3\ ^{[6]}(Mg+Fe) + 3\ ^{[4]}Si \qquad (5)$$

$$^{[12]}Ba + 2\ ^{[6]}Ti + 3\ ^{[4]}Al = {}^{[12]}K + {}^{[12]}Na + 3\ ^{[6]}(Mg+Fe+Mn) + 3\ ^{[4]}Si. \qquad (6)$$

Based on the detailed regression analysis, we attribute the exchange mechanism in the Mezitler biotites to the following equation (7) with negligible depart from a 1:1 slope (Fig. 6d).

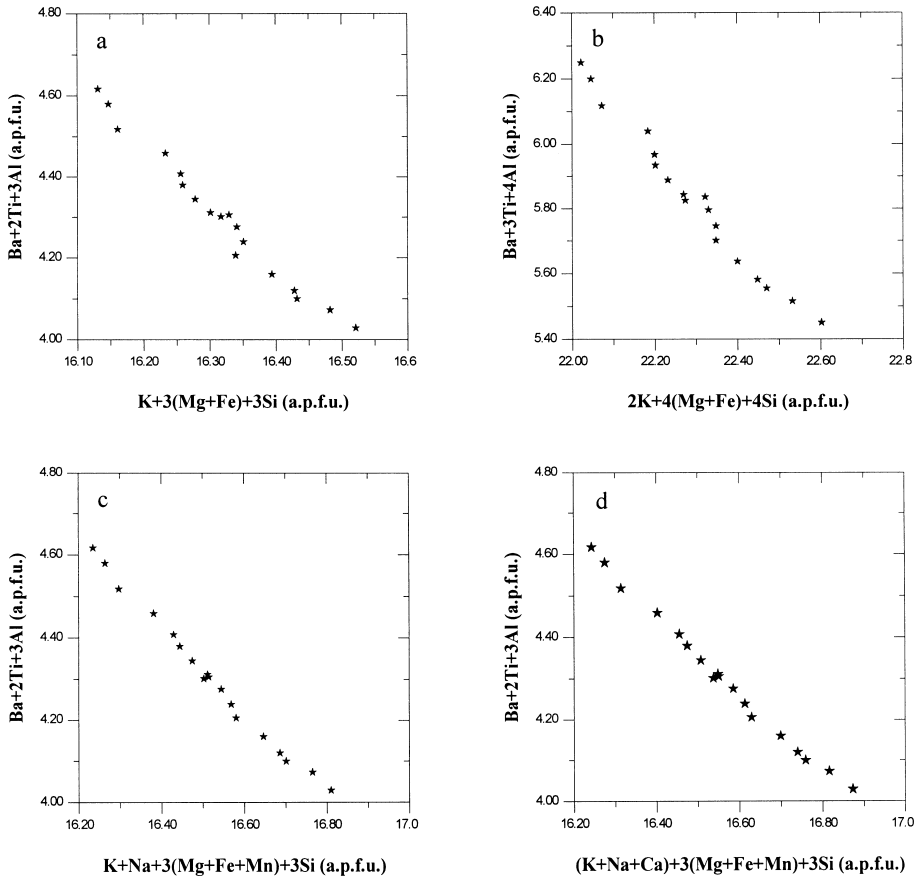

Fig. 6. Trend of Mezitler micas on a) Ba+2Ti+3Al vs. K+3(Mg+Fe)+3Si, b) Ba+3Ti+4Al vs. 2K+4(Mg+Fe)+4Si, c) Ba+2Ti+3Al vs. K+Na+3(Mg+Fe+Mn)+3Si, and d) Ba+2Ti+3Al vs. (K+Na+Ca)+3(Mg+Fe+Mn)+3Si diagrams.

$$^{[12]}\text{Ba} + 2\,^{[6]}\text{Ti} + 3\,^{[4]}\text{Al} = {}^{[12]}(\text{K+Na+Ca}) + 3\,^{[6]}(\text{Mg+Fe+Mn}) + 3\,^{[4]}\text{Si}. \quad (7)$$

These substitutions given here are common for most of Ba-rich micas in magmatic rocks.

Ti substitutions

The behavior of Ti in Ba- and Ti-rich micas depends on Ti valency and occupancy. Correlations between Ti vs. (Si+Al) and Ti vs. (Fe+Mg) are $r = 0.51$ and $r = 0.46$ respectively. This suggests that Ti may not enter the tetrahedral site by the following mechanism:

$$^{[4]}\text{Ti} = {}^{[4]}\text{Si}. \quad (8)$$

The mineral chemistry of Mezitler biotites shows full tetrahedral site and therefore other substitutions may be involved. The Ti substitution in the tetrahedral and octahedral sites is given by the mechanism shown below, with the correlation coefficient of $r = 0.95$.

$$^{[4]}\text{Al} + {}^{[6]}\text{Ti} = {}^{[4]}\text{Si} + {}^{[6]}\text{Al}. \quad (9)$$

Although the substitution mechanism shown below is theoretically possible, it seems inapplicable for the Mezitler biotites because of the inrelation correlation between Ti and (Mg+Fe).

$$^{[6]}\text{Ti} + {}^{[6]}\square = 2\,^{[6]}(\text{Mg,Fe}^{2+}). \quad (10)$$

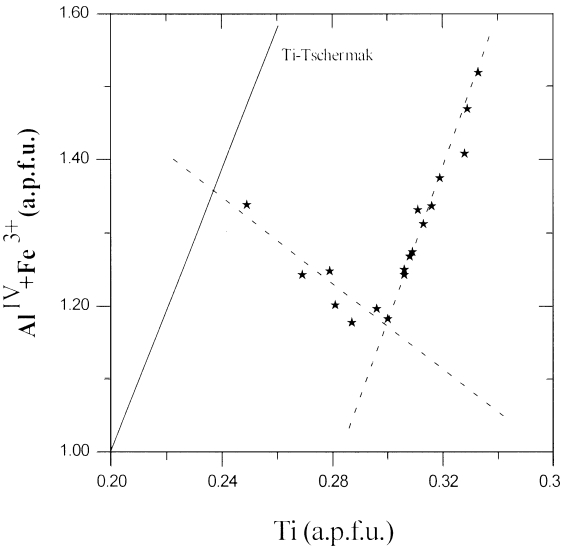

Fig. 7. Plot of ($Al^{IV}+Fe^{3+}$) vs. Ti for Mezitler micas, with a line showing a Ti-Tschermakite substitution.

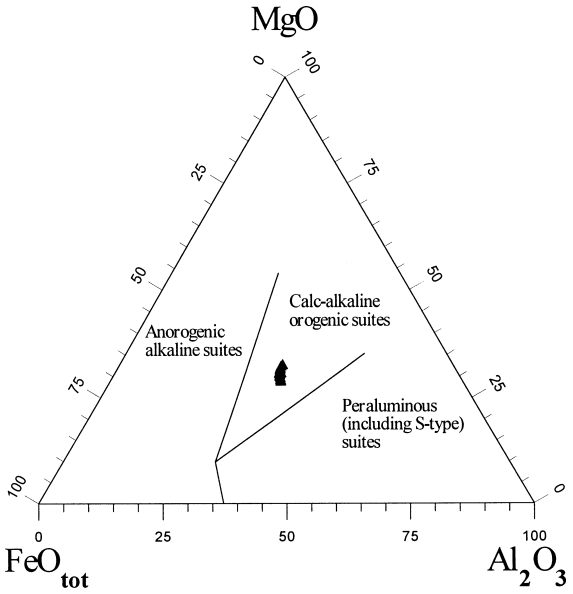

Fig. 8. Plot of Mezitler biotites on FeO_t-MgO-Al_2O_3 ternary biotite discrimination diagram (from Abdel-Rahman, 1994).

In considering Ti in the octahedral site Ti-Tschermakite substitution can be written as:

$$^{[6]}Ti + 2^{[4]}(Al,Fe^{3+}) = {}^{[6]}(Mg,Fe^{2+}) + 2\ {}^{[4]}Si. \quad (11)$$

The substitution mechanism of Mezitler micas with this scheme shows parallel trend to a line representing Ti-Tschermakite substitution (Fig. 7).

Petrological considerations

According to the statistical approach of Abdel-Rahman (1994) on biotites in various igneous rock types, three compositionally distinct fields were defined. These are biotites in alkaline anorogenic suites, biotites in peraluminous suites and biotites in calc-alkaline orogenic suites. The chemical composition of Mezitler biotites on the ternary discrimination diagram of FeO_t-MgO-Al_2O_3 suggests that host rocks are members of the calc-alkaline orogenic suites that are typically found in a subduction environment (Fig. 8). Based on experimental study, Guo and Green (1990) showed that the amount of Ba in the mica structure could be determined by the Ti solubility. They discussed that the partitioning of Ba between mica and liquid is controlled by the compositional effect compared to thermal conditions. They also proposed that increased pressure decrease the amount of Ba entering in mica relative to melt. The Ba-bearing biotites from Mezitler rocks are generally found in the groundmass and as phenocrysts. This indicates that micas are formed at different temperature intervals. The lack of important differences in BaO contents between groundmass and phenocrysts, and the absence of regular zoning in micas for BaO and TiO_2 contents does not point out if temperature or fractionation processes played an important role in Ba-enrichment in the Mezitler micas. The average Mg# of micas is 0.60, which indicates moderate degrees of fractionation.

The presence of coexisting biotite, alkali feldspar and iron-titanium oxide minerals in the studied samples from Mezitler area provide the basis for tentatively estimating some extensive parameters, such as $f(O_2)$ and $f(H_2O)$. In the Fe^{2+}-Fe^{3+}-Mg diagram of Wones and Eugster (1965) biotite compositions fall between the quartz-fayalite-magnetite (QFM) and Ni-NiO (NNO) oxygen fugacity buffers (Fig. 9). The oxygen fugacity can

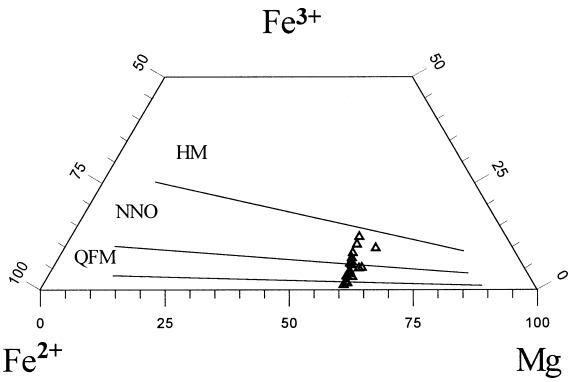

Fig. 9. The composition of micas from Mezitler in the Fe^{2+}-Fe^{3+}-Mg diagram of Wones and Eugster (1965). Lines represent mica composition in equilibrium with oxygen buffers, hematite-magnetite (HM), nickel-nickel oxide (NNO), quartz-fayalite-magnetite (QFM).

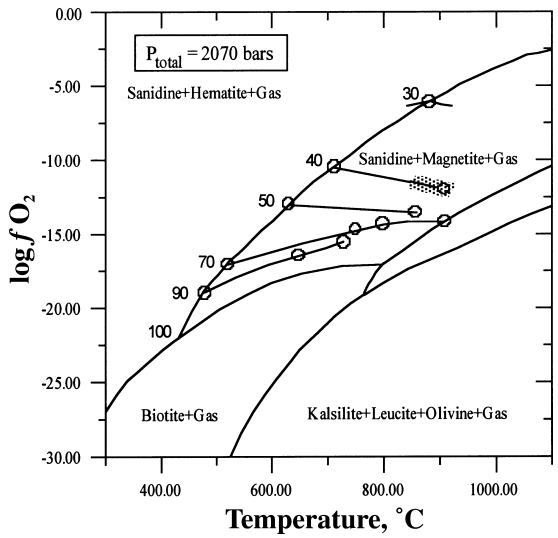

Fig. 10. Position of the Mezitler micas on log f (O_2)-T diagram for the biotite+sanidine+magnetite+gas equilibrium at P_{tot} = 2070 bars (from Wones and Eugster, 1965).

also be evaluated from the calibrated curves of Wones and Eugster (1965) in *f* (O_2)-*T* space. The Mezitler volcanic rocks equilibrated at an oxygen fugacity between $10^{-11.89}$ and $10^{-11.95}$, which shows the conditions between NNO and QFM buffers for the temperatures of crystallization interval between 880° and 920°C. The solubility of Ti and Ca in biotite generally increases with increasing temperature (Shau *et al.*, 1991). Sagenitic biotites in some thin sections also support the present biotites have had a relatively high temperature of crystallization. Calculations made using the BIOTERM software (Yavuz and Öztaş, 1997) indicated that the Mezitler micas were crystallized at *f* (H_2O) between 0.4 and 1.0 kilobars. Hence, it is possible to suggest that the Mezitler Ba-bearing biotites formed at relatively high temperature, high oxygen fugacity, low total pressure, and low *f* (H_2O). These results are consistent with crystallization under conditions of high temperature and low pressure for the high Ti and Ba contents of biotite (Edgar *et al.*, 1976, Trønnes *et al.*, 1985; Guo and Green, 1990; Henderson and Foland, 1996).

Barium, as an incompatible element, is characteristic of mantle-derived magmas, such as lamproites and alkaline potassic rocks (Jaques *et al.*, 1986; Thompson *et al.*, 1997). However, it is strongly compatible in mica and enters the structure during the earliest stage of crystallization (Henderson, 1982; Shaw and Penczak, 1996). The presence of Ba-bearing biotites suggests that the Mezitler volcanic rocks and hosted hydrothermal Mn-oxide and barite deposits formed relatively shallow and oxic environments. In that way, micas from the Mezitler area may be comparable to those micas of the Yindongzi-Daxigou Pb-Zn-Ag deposits (Jiang *et al.*, 1996) except for substitution mechanisms. It is assumed that Ba entered the mica structure at the earlier stage of crystallization as the source magma was generated in a subduction-enriched sub-continental lithospheric mantle. Micas in this type of environment appear to contain lower Ba and Ti contents compared to high Ba- and Ti-bearing micas in relatively thin, oceanic lithosphere, passing over a hot mantle plume, such as the islands of Hawaii (Mansker *et al.*, 1979), Cape Verde (Furnes and Stillman, 1987) and Gough (Le Roex, 1985). Comparison of the Mezitler micas that with the other micas from different geologic environments is shown in Fig. 11. It is clear from this figure that the Mezitler micas, which found in calc-alkaline magmatic rocks over-

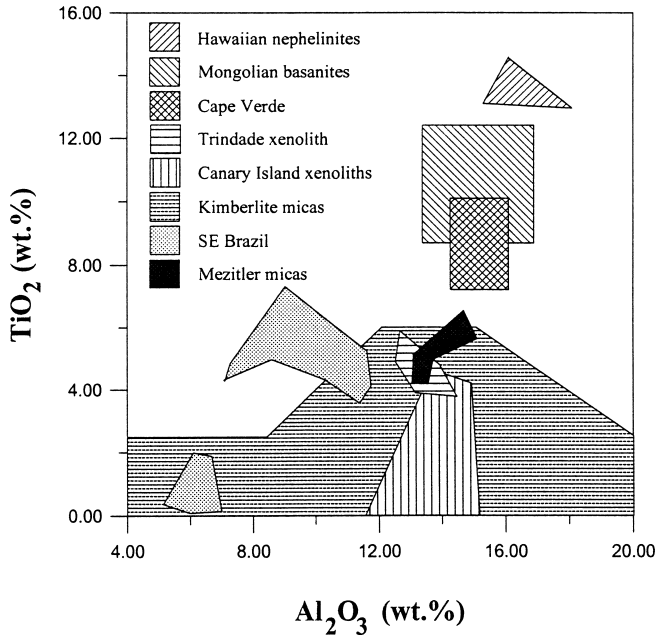

Fig. 11. Comparison of compositional variations of micas from the Mezitler area those with other micas from different geological environments. Hawaiian nephelinites (Mansker et al., 1979); Mongolian basanites (Ryabchikov et al., 1982); Cape Verde (Furnes and Stillman, 1987); SE Brazil (Meyer et al., 1994; Leonardos et al., 1991); Kimberlite micas (Mitchell, 1986); Canary Islands (Wulff-Pedersen et al., 1996).

lap the field for micas from Ilha da Trindade, South Atlantic (Greenwood, 1998) and lie on a trend parallel to those for metazomatic phlogopites from Canary Island xenoliths (Wulff-Pedersen *et al*., 1996).

CONCLUSIONS

The calc-alkaline volcanic rocks in western Turkey are enriched in the large ion lithophile (LIL) elements. Geochemical studies point out a hybrid origin, with contamination of mantle-derived magmas to the crustal materials (Yılmaz, 1989, 1997). Biotites from the calc-alkaline Mezitler volcanic rocks are moderately enriched in Ba and Ti. These micas contain up to 1.72 wt.% BaO and 5.90 wt.% TiO_2. The presence of barium in the mica structure can be explained by two factors the geometry of the inter-layer cation site and the mechanism of charge compensation, respectively. It seems that the incorporation of Ba into the mica structure is controlled by the Ba + 2Ti + 3Al = (K+Na+Ca) + 3(Mg+Fe+Mn) + 3Si coupled complex substitution mechanism.

Textural and petrological studies indicate that biotite in the Mezitler volcanic rocks is an early phase, which crystallized from calc-alkaline melts at near-surface pressures. Relatively low to moderate BaO contents (0.40–1.72 wt.%) in biotites from the studied area can also be explained by the entry of negligible amounts of Ba into the early-formed biotite phenocrysts. The crystallizing residual melt is enriched in Ba and, thus, vein-type barite deposits were formed in the volcanic rocks depending on later hydrothermal processes. The high content of micas in the alkali-rich rocks may be explained by late-magmatic processes during the mica crystallization. According to the experimentally calibrated curve of Wones and Eugster (1965) for biotite + K-feldspar + magnetite equilibrium, the Mezitler rocks equilibrated at an average $f\,(O_2)$ of $10^{-11.92}$ for a temperature of crystallization of 900°C, which corresponds to conditions between NNO and QFM buffers. This shows

that Ba-bearing micas formed at relatively high temperature, high $f(O_2)$, and low $f(H_2O)$. These results are consistent with a low to moderate Ba- and Ti-bearing mica that are thought to have been formed by magmas in a subduction-enriched subcontinental lithospheric mantle.

Acknowledgments—We would like to thank A. E. Lalonde, Université d' Ottawa, Ottawa, Ontario, for his advice and comments on earlier draft of the manuscript. We thank F. Koller, University of Vienna, and A. Mogessie, University of Graz, for their constructive reviews of the manuscript. We also grateful to C. Koeberl for his careful reading of the manuscript and editorial assistance.

REFERENCES

Abdel-Rahman, A. M. (1994) Nature of biotites from alkaline, calc-alkaline, and peraluminous magmas. *J. Petrol*. **35**, 525–541.

Altunkaynak, Ş. and Yılmaz, Y. (1995) The Mount Kozak magmatic complex, western Anatolia. *J. Volcanol. Geotherm. Res*. **85**, 211–231.

Bigi, S., Brigatti, M. F., Mazzucchelli, M. and Rivalenti, G. (1993) Crystal chemical variations in Ba-rich biotites from gabbroic rocks of lower crust (Ivrea Zone, NW Italy). *Contrib. Mineral. Petrol*. **113**, 87–99.

Bol, L. C. G. M., Bos, A., Sauter, P. C. C. and Jansen, J. B. H. (1989) Barium-titanium-rich phlogopites in marbles from Rogaland, southwest Norway. *Am. Mineral*. **74**, 439–447.

Dymek, R. F. (1983) Titanium, aluminium and interlayer cation substitutions in biotite from high-grade gneisses, West Greenland. *Am. Mineral*. **68**, 880–899.

Edgar, A. D. (1992) Barium-rich phlogopite and biotite from some Quaternary alkali mafic lavas, west Eifel, Germany. *Eur. J. Mineral*. **4**, 321–330.

Edgar, A. D., Green, D. H., Hibberson and W. O. (1976) Experimental petrology of a highly potassic magma. *J. Petrol*. **17**, 339–356.

Ercan, T., Satır, M., Kreuzer, H., Türkecan, A., Günay, E., Çevikbaş, A., Ateş, M. and Can, B. (1985) Interpretation of new chemical isotopic and radiometric data on Cenozoic volcanics of western Anatolia. *Bull. Geol. Soc. Turkey* **28**, 121–136 (in Turkish).

Ersoy, H. (1989) The geology of iron-bearing manganese mineralization from Balıkesir-Bigadiç-Mezitler-Tumanpınarı. MTA Rep. 8716 (in Turkish).

Foley, S. F. (1989) Experimental constraints on phlogopite chemistry in lamproites: 1. The effect of water activity and oxygen fugacity. *Eur. J. Mineral*. **1**, 411–426.

Foley, S. F. (1990) Experimental constraints on phlogopite chemistry in lamproites: 2. Effect of pressure-temperature variations. *Eur. J. Mineral*. **2**, 327–341.

Foster, M. D. (1960) Interpretation of the composition of trioctahedral micas. *U.S. Geol. Surv. Prof. Pap*. **354B**, 1–49.

Furnes, H. and Stillman, C. J. (1987) The geochemistry and petrology of an alkaline lamprophyre sheet intrusion complex on Maio, Cape Verde Republic. *J. Geol. Soc. London* **144**, 227–241.

Genç, Ş. C. (1995) Evolution of the Bayramiç magmatic complex, northwestern Anatolia. *J. Volcanol. Geotherm. Res*. **85**, 233–249.

Genç, Ş. C. and Yılmaz, Y. (1995) Post-collisional Eocene magmatic activity of NW Anatolia. *Terra Nova 7 Abst. Suppl*. **1**, 181.

Grapes, R. H. (1993) Barian mica and distribution of barium in metacherts and quartzofeldspathic schist, Southern Alps, New Zealand. *Mineral. Mag*. **57**, 265–272.

Greenwood, J. C. (1998) Barian-titanian micas from Ilha da Trindade, South Atlantic. *Mineral. Mag*. **62**, 687–695.

Guo, J. and Green, T. H. (1990) Experimental study of barium partitioning between phlogopite and silicate liquid at upper-mantle pressure and temperature. *Lithos* **24**, 83–95.

Gültekin, A. H. and Örgün, Y. (1999) Geochemistry of andesite-hosted vein-type Mn-Ba mineralizations, Bigadiç, Balıkesir, Turkey. *Progress in Mining and Oilfield Chemistry* (Lakatos, I., ed.), 239–248, Challenges of an Interdisciplinary Science, Akadémiai Kiadó, Budapest.

Gültekin, A. H., Örgün, Y. and Yavuz, F. (1998) The geological, mineralogical and geochemical characteristics of Tumanpınarı (Balıkesir-Dursunbey) Fe-Mn mineralization. *Geol. Bull. Turkey* **41**, 13–30 (in Turkish).

Harlow, G. E. (1995) Crystal chemistry of barian enrichment in micas from metasomatized inclusions in serpentinite, Motagua Fault Zone, Guatemala. *Eur. J. Mineral*. **7**, 775–789.

Henderson, C. M. B. and Foland, K. A. (1996) Ba- and Ti-rich primary biotite from the Brome alkaline igneous complex, Monteregian Hills, Quebec: mechanisms of substitution. *Can. Mineral*. **34**, 1241–1252.

Henderson, P. (1982) *Inorganic Geochemistry*. Pergamon Press, Oxford, U.K., 353 pp.

Jacobs, D. C. and Parry, W. T. (1979) Geochemistry of biotite in the Santa Rita porphyry copper deposit,

New Mexico. *Econ. Geol*. **74**, 860–887.

Jaques, A. L., Lewis, C. D. and Smith, C. B. (1986) The kimberlites and lamproites of Western Australia. *Geol-Surv. Western Australia Bull*. **132**, 268 pp.

Jiang, S.-Y., Palmer, M. R., Li, Y.-H. and Xue, C.-J. (1996) Ba-rich micas from the Yindongzi-Daxigou Pb-Zn-Ag and Fe deposits, Qinling, northwestern China. *Mineral. Mag*. **60**, 433–445.

Karacık, Z. and Yılmaz, Y. (1995) Geology of the ignimbrites and the associated volcano-plutonic complex of the Edina area, northwestern Anatolia. *J. Volcanol. Geotherm. Res*. **85**, 251–264.

Le Maitre, R. W. (1989) *A Classification of Igneous Rocks and Glossary of Terms*. Blackwell, Oxford, 193 pp.

Leonardos, O. H., Ulbrich, M. N. and Gaspar, J. C. (1991) The Mata da Corda volcanic rocks. *Field Guidebook. 5th International Kinberlite Brasilia*, DF: CPRM, Special Publication 3/91, 17–24.

Le Roex, A. P. (1985) Geochemistry, mineralogy and magmatic evolution of the basaltic and trachytic lavas from Gough Island, South Atlantic. *J. Petrol*. **26**, 149–186.

Mansker, W. L., Ewing, R. C. and Keil, K. (1979) Barian-titanian biotites in nephelinites from Oahu, Hawaii. *Am. Mineral*. **64**, 156–159.

Meyer, H. O. A., Garwood, B. L., Svisero, D. P. and Smith, C. B. (1994) Alkaline intrusions in western Minas Gerais, Brazil. *Proceedings of the 5th International Kimberlite Conference, Araxá* (Leonardos, O. H., Meyer, H. O. A. and Gasper, J. C., eds.), 140–155, DF: CPRM, Special Publication, Brasília.

Mitchell, R. H. (1981) Titaniferous phlogopites from the Leucite lamproites of the West Kimberley area, Western Australia. *Contrib. Mineral. Petrol*. **76**, 243–251.

Mitchell, R. H. (1986) *Kimberlites, Mineralogy, Geochemistry and Petrology*. Plenum, New York, 442 pp.

Rieder, M. (2001) Mineral nomenclature in the mica group: the promise and the reality. *Eur. J. Mineral*. **13**, 1009–1012.

Ryabchikov, L. D., Kovalenko, V. I., Dikov, Y. P. and Vladykin, N. V. (1982) Titaniferous micas from the mantle: composition, structure, formation conditions, and possible role in the production of potassic alkali magmas. *Geochem. International* **18**, 124–137.

Shau, Y.-H., Yang, H.-Y. and Peacor, D. R. (1991) On oriented titanite and rutile inclusions in sagenitic biotite. *Am. Mineral*. **76**, 1205–1217.

Shaw, C. S. J. and Penczak, R. S. (1996) Barium- and titanium-rich biotite and phlogopite from the western and eastern gabbro, Coldwell Alkaline Complex, northwestern Ontario. *Can. Mineral*. **34**, 967–975.

Solie, D. N. and Su, S.-C. (1987) An occurrence of Ba-rich micas from the Alaska Range. *Am. Mineral*. **72**, 995–999.

Speer, R. (1984) Micas in igneous rocks. *Reviews in Mineralogy: Micas* (Bailey, S. W., ed.), 299–349, Mineralogical Society of America.

Thompson, R. N., Velde, D., Leat, P. T., Morrison, M. A., Mitchell, J. G., Dickin, A. P. and Gibson, S. A. (1997) Oligocene lamproite containing an Al-poor, Ti-rich biotite, Middle Park, northwest Colorado, USA. *Mineral. Mag*. **61**, 557–572.

Tischendorf, G., Gottesmann, B., Förster, H. J. and Trumbull, R. B. (1997) On Li-bearing micas: estimating Li from electron microprobe analyses and improved diagram for graphical representation. *Mineral. Mag*. **61**, 809–834.

Tracy, R. J. (1991) Ba-rich micas from the Franklin Marble, Lime Crest and Sterling Hill, New Jersey. *Am. Mineral*. **76**, 1683–1693.

Trønnes, R. G., Edgar, A. D. and Arima, A. (1985) A high-pressure high-temperature study of TiO_2 solubility in Mg-rich phlogopite: implications to phlogopite chemistry. *Geochim. Cosmochim. Acta* **49**, 2323–2329.

Velde, D. (1979) Trioctahedral micas in melilite-bearing eruptive rocks. *Carn. Inst. Washington Yearb*. **78**, 468–475.

Wagner, C. and Velde, D. (1986) The mineralogy of K-richterite-bearing lamproites. *Am. Mineral*. **71**, 17–37.

Wendlandt, R. F. (1977) Barium phlogopites from Haystacks Butte, Highwood Mountains, Montana. *Carnegie Institution of Washington Year Book* **76**, 534–539.

Winchester, J. A. and Floyd, P. A. (1977) Geochemical classification of different magma series and their differentiation products using immobile elements. *Chem. Geol*. **20**, 325–343.

Wones, D. R. and Eugster, H. P. (1965) Stability of biotite: experiment, theory, and application. *Am. Mineral*. **50**, 1228–1272.

Wulff-Pedersen, E., Neuman, E. R. and Jensen, B. B. (1996) The upper mantle under La Palma, Canary Islands: formation of Si-K-Na-rich melt and its importance as a metasomatic agent. *Contrib. Mineral. Petrol*. **125**, 113–139.

Yavuz, F. (1999) A revised program for microprobe-derived amphibole analyses using the IMA rules. *Computers & Geosciences* **25**, 909–927.

Yavuz, F. (2001a) LIMICA: A program for estimating Li from electron-microprobe mica analyses and classifying triochtahedral micas in term of composition and octahedral site occupancy. *Computers & Geosciences* **27**, 215–227.

Yavuz, F. (2001b) PYROX: A computer program for the IMA pyroxene classification and calculation scheme. *Computers & Geosciences* **27**, 97–107

Yavuz, F. (2002) Evaluating micas in petrologic and metallogenic aspect: I—definitions and structure of the computer program MICA^{+}. *Computers & Geosciences* (in press).

Yavuz, F. and Öztaş, T. (1997) BIOTERM-A program for evaluating and plotting microprobe analyses of biotite from barren and mineralized magmatic suites. *Computers & Geosciences* **23**, 897–907.

Yılmaz, Y. (1989) An approach to the origin of volcanic rocks of western Turkey. *Tectonic Evolution of the Tethyan Region* (Sengör, A. M. C., ed.), 159–189, Kluwer.

Yılmaz, Y. (1997) Geology of western Anatolia.—Active Tectonics of Northwestern Anatolia. The Marmara Poly-Project, ETH Zurich, 31–53.

Yui, T.-F., Shen, P. and Liu, H.-H. (2001) Titanite inclusions in altered biotite from granitoids of Taiwan: microstructures and origins. *J. Asian Earth Sci*. **19**, 165–175.

Zhang, M., Suddaby, P., Thompson, R. N. and Dungan, M. A. (1993) Barian titanian phlogopite from potassic lavas in northeast China: Chemistry, substitution, and parageneses. *Am. Mineral*. **78**, 1056–1065.